Analysis of timber trusses using semi-rigid joints

D. I. MASSÉ[1] and J. J. SALINAS[2]

[1]*Engineering and Statistical Research Centre, Research Branch, Agriculture Canada, Ottawa, Ontario K1A 0C6; and*
[2]*Department of Civil Engineering, Carleton University, Ottawa, Ont. K1A 5B6.* *Contribution no. [1]I-720. received 28 August 1986, accepted 26 May 1987.*

Massé, D. I. and Salinas, J. J. 1988. **Analysis of timber trusses using semi-rigid joints.** Can. Agric. Eng. **30**: 111–124. Based on the "Canada Plan Service" roof truss test series, it was evident that the strength predicted by traditional design methods did not agree completely with the experimental results. These comparisons showed that there was a need for a more advanced method of analysis which considered the effects of secondary stresses due to truss deflection and joint slip. In this paper, a theoretical analysis of the joint stiffness is compared with experimental results from full-scale truss joint tests. The information is then used with a stiffness analysis computer program to give the stress and deformation at any point within the truss. Finally, these results are compared with experimental data from further tests on full-scale roof trusses. Since there was good agreement between theoretical and experimental results, the standard Canada Plan Service (CPS) truss designs should be reanalyzed accordingly.

INTRODUCTION

Multi-laminated nailed joints have been introduced in the Canada Plan Service (CPS) by Turnbull et al. (1981) to provide heavy duty hand-nailed roof trusses suitable for building at the farm site.

As shown in Fig. 1, the typical joint is made from double S-P-F no. 2 lumber members connected with three gussets — two 12.5-mm exterior sheathing Douglas Fir (D-F) plywood gussets on the outside faces of the joint and one 0.95-mm galvanized steel gusset in the middle. The joints are fastened with 4 × 102-mm Stelco "Ardox" spiral nails driven from each side. The following advantages are obtained in using this type of connection:

(1) The steel gusset increases the number of shear planes from two to four, thereby reducing the total number of nails required.

(2) The heavy duty trusses can be spaced at the same spacing as the poles and bear directly on them in order to eliminate the construction of a plate beam otherwise required for closer truss spacing.

The CPS multi-laminated nailed joint trusses have been designed by the following traditional approximate design approach: the axial forces were determined by assuming that the members ends were pinned; the upper chord moments were found by considering the upper chord to be pinned at the heel joint, continuous over the web connections and pinned at the ridge; and the web members and the lower chord were designed for axial forces only. The gussets were designed to provide enough area for the total number of nails, respecting the minimum nail spacing, and enough cross section to transfer shear and axial forces.

In order to verify the design assumptions, Turnbull et al. (1983a) load tested two families of multi-laminated nail joint trusses. The first was the double slope configuration with equal upper chord spans. For this type of truss, according to the traditional analysis method, the maximum combined stress ratio occurred in the upper chord exterior span. Therefore truss failure would be expected to occur in that member. Five trusses were load tested but none failed at that location. Two failures occurred in the lower chord member exterior span splice and three failures occurred in the lower chord interior span splice. The other family of trusses tested were the single slope multi-laminated trusses with an upper chord span length adjusted to equalize the combined stress ratio. Again the traditional analysis method predicted that the maximum stress ratio would occur in the upper chord spans and that truss failure was expected to occur at random in the upper chord. Six trusses were tested and upper chord failure did not occur. Two buckling failures occurred in the long compressive web member and four failures occurred in the lower chord nailed splice connections.

Truss failure did not occur at the location predicted by the traditional analysis method for either series of tests. It was felt that this was possibly due to the fact that the effect of secondary stresses due to member end-rotation and deformation, which are a function of the joint axial and rotational stiffness, were not considered.

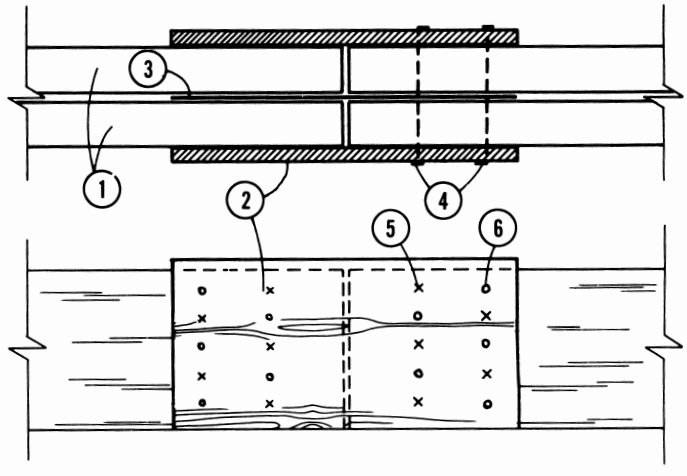

1 38 mm thick S.P.F. #2
2 12.5 mm exterior sheathing Douglas fir plywood
3 0.95 mm galvanized steel gusset
4 4 x 102 mm common spiral nails
5 denote nails from other side
6 denote nails from this side

Figure 1. Typical multi-laminated nailed joints.

The primary objective of this study was to provide a more refined structural analysis of the multi-laminated nailed joint wooden roof trusses than was used previously. An improved analysis method would make it possible to predict more accurately the truss behavior and optimize the designs. It was also desirable to reduce the number of full-scale tests required to verify truss performance when the theoretical structural analysis was based on approximate assumptions.

In order to develop a more accurate analysis it was necessary to consider the joints more realistically. To achieve this, more information was needed on axial and rotational stiffness of multi-laminated nailed wood joints.

A theoretical analysis of truss joint stiffness was carried out in this investigation and compared with results obtained experimentally from joint tests. Good agreement was observed. The theoretical results were then used to carry out an investigation of the effect of joint stiffness on the stress distribution and deformation at any location within the truss. Results of this latter investigation were compared with the results from tests on full-scale multi-laminated trusses.

ANALYSIS OF JOINT STIFFNESS

Axial tests

In order to develop an accurate analog model it was necessary to study joint axial and rotational stiffness. A series of joint tests were conducted to determine the stiffness of a multi-laminated nailed joint subjected to an axial load applied parallel to the grain. Ten multi-laminated nailed joints made with green lumber were load tested at a moisture content of 17% to simulate field conditions and to reduce the friction between the lumber members and the gussets (Fig. 1). Figure 2 shows the joint details and the instrumentation. The joints were tested in a Tinius Olsen 1800 kN universal testing machine at a loading rate of 4.5 kN/min.

Figure 3 shows the mean load/displacement data of one-half of the joint. Each point on the curve represents the mean of 10 tests. The coefficient of variation for different points ranged from 3 to 10%. As shown, there is a nonlinear relationship between the joint load and the joint deformation. Also shown in Fig. 3 is an exponential curve fitted to data. In order to get a close fit, the parameters of the power function change at a joint deformation of 0.5 mm.

The load-slip curve for a single nail was derived from the test results by assuming a uniform distribution among all nails. The load corresponding to a specific displacement was divided by the total number of nails on one side of the joint. Figure 4 shows the load-displacement curve for a single nail in a multi-laminated nailed joint and the corresponding exponential curve of best fit. This exponential function was later used to estimate the axial, transverse and rotational stiffnesses of multi-laminated nailed joints.

Rotational stiffness

Theoretical

The theoretical expression to determine the rotational stiffness of a multi-laminated nailed joint was developed using the estimated load-slip curve for a single nail and the modified torsion formula developed by Perkins (1962). It was assumed that the load/displacement relationship for a nail measured parallel to the grain could be used for all directions in the wood.

$$M = \sum_{i=1}^{n} m_i$$

$$m_i = 4223(2\theta R_i)^{0.507} R_i \quad \text{for } \theta R_i < 0.5$$

$$m_i = 4152(2\theta R_i)^{0.349} R_i \quad \text{for } \theta R_i > 0.5$$

M = total resisting moment of the joint (N.mm),
m_i = moment resisted by a single nail,
θ = joint rotation radians
R_i = distance from center of resistance to the nail (mm).

Experimental

To determine if the theoretical expression for the moment-rotation relationship was accurate for multi-laminated nailed joints, an experimental investigation of the rotational stiffness of a multi-laminated nailed joint was carried out. Ten joints were built with the same material and same procedure as those tested in tension. The only difference was that the lumber size used

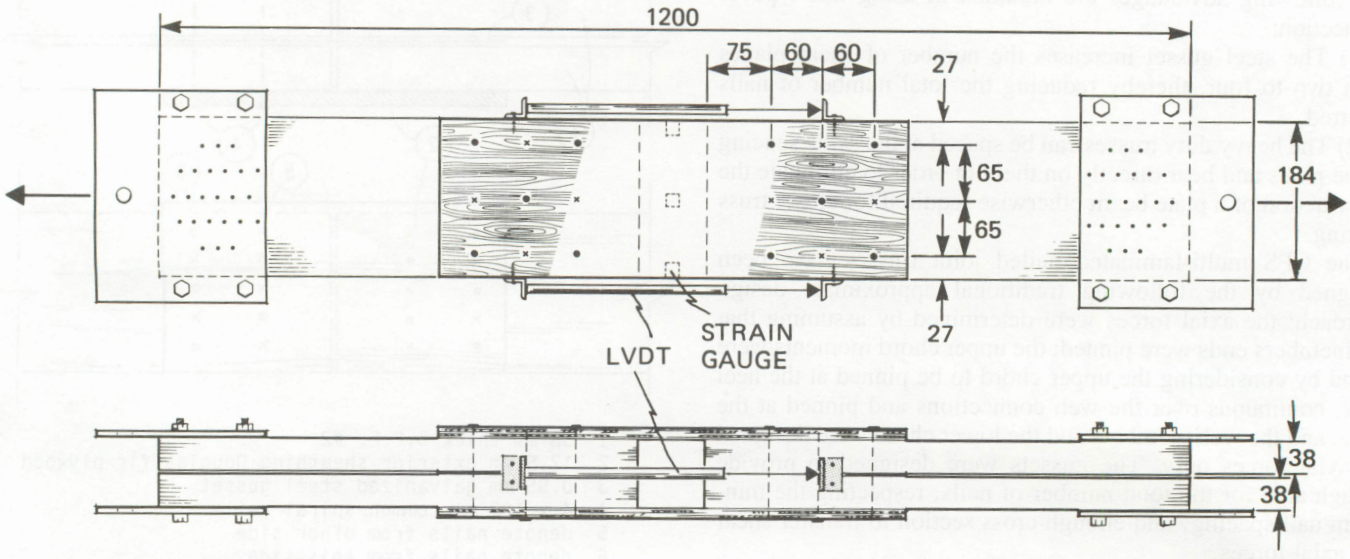

Figure 2. Details of tension specimens, showing nailed plywood gussets, steel gusset, wood gripping system and the two LVDTs (dimensions in mm).

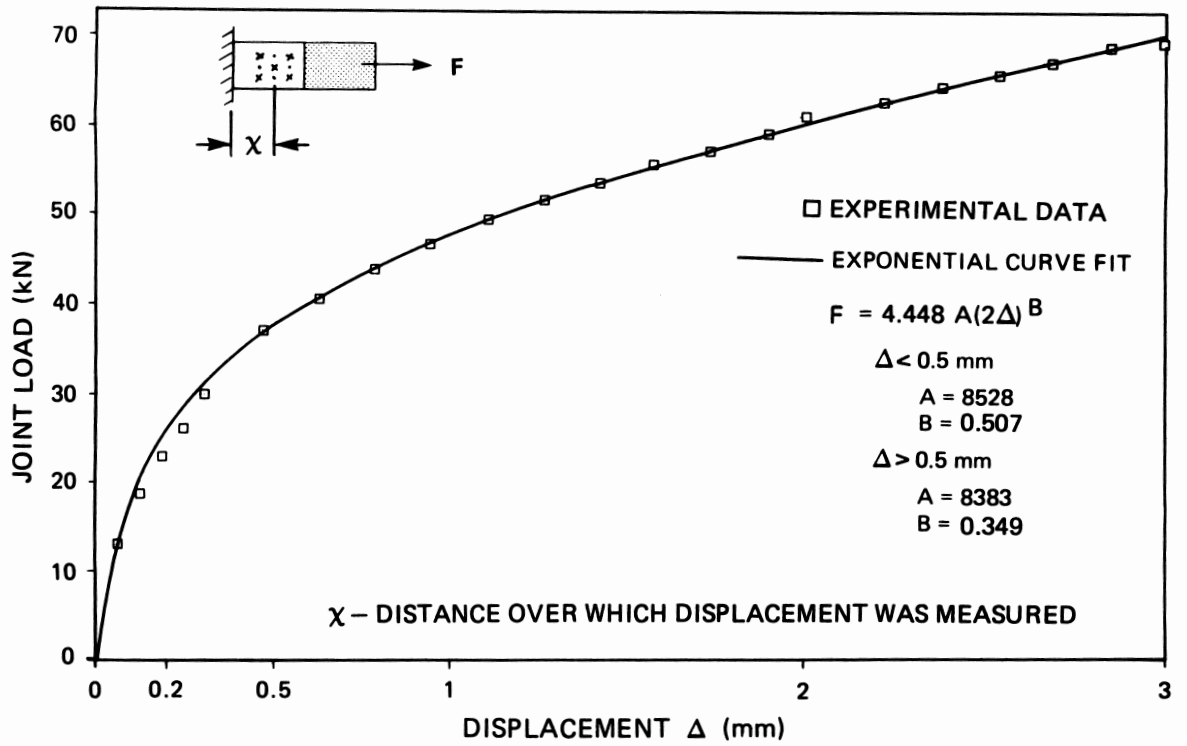

Figure 3. Mean load/displacement data of one-half of the tension specimen and fitted exponential curve (Massé 1985).

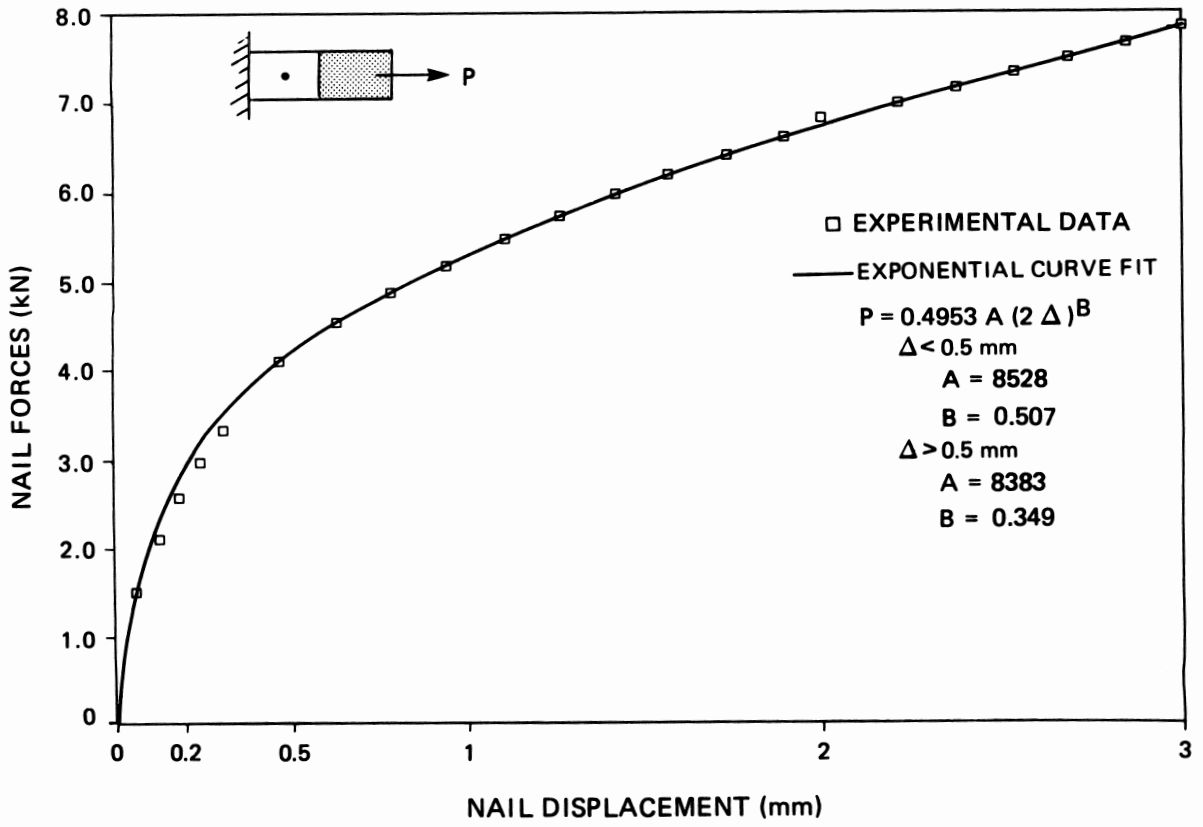

Figure 4. Mean load/displacement curve for a single nail derived from test results (Massé 1985).

was 38 × 235 mm instead of 38 × 184 mm. The joints were built with a 6-mm end gap in order to measure only the rotational stiffness of the nailing pattern.

Figure 5 shows the joint details as well as the two-point loading pattern used in order to get a constant bending moment and zero shear throughout the joint between the applied loads. Two LVDT transducers at the mid-span of the joint measured the vertical displacement of the timber members. The specimens were load tested on a Tinius Olsen 1800 kN Universal Testing Machine at a loading rate of 4.5 kN/min. Figure 6 shows the curve of the average test results. Each point on the curve represents the mean of 10 tests. The coefficient of variation for

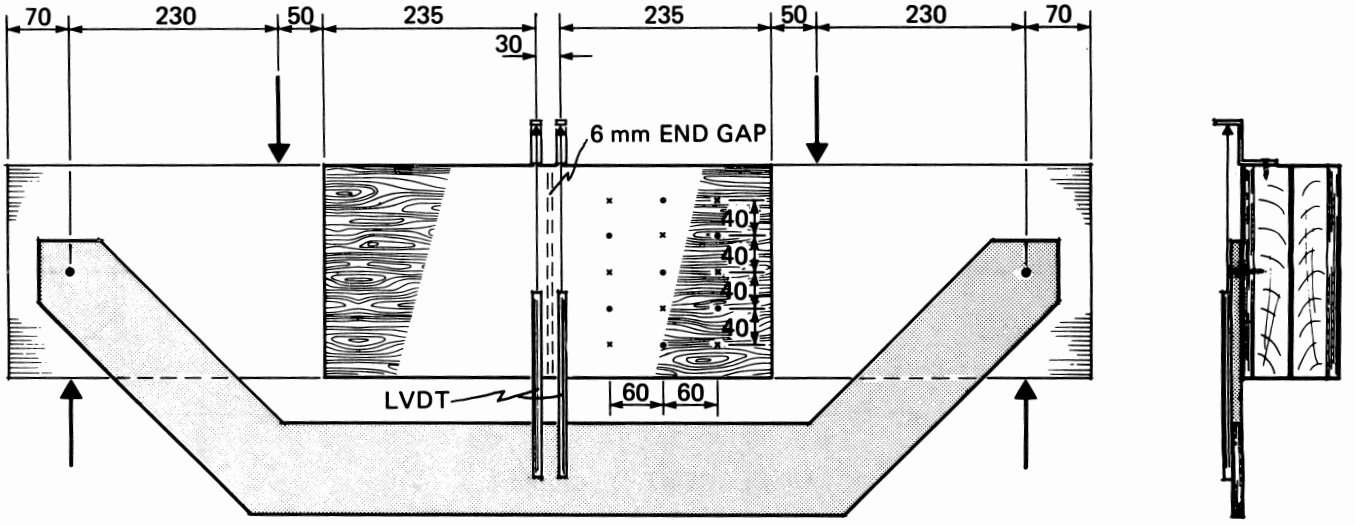

Figure 5. Details of test specimen in bending.

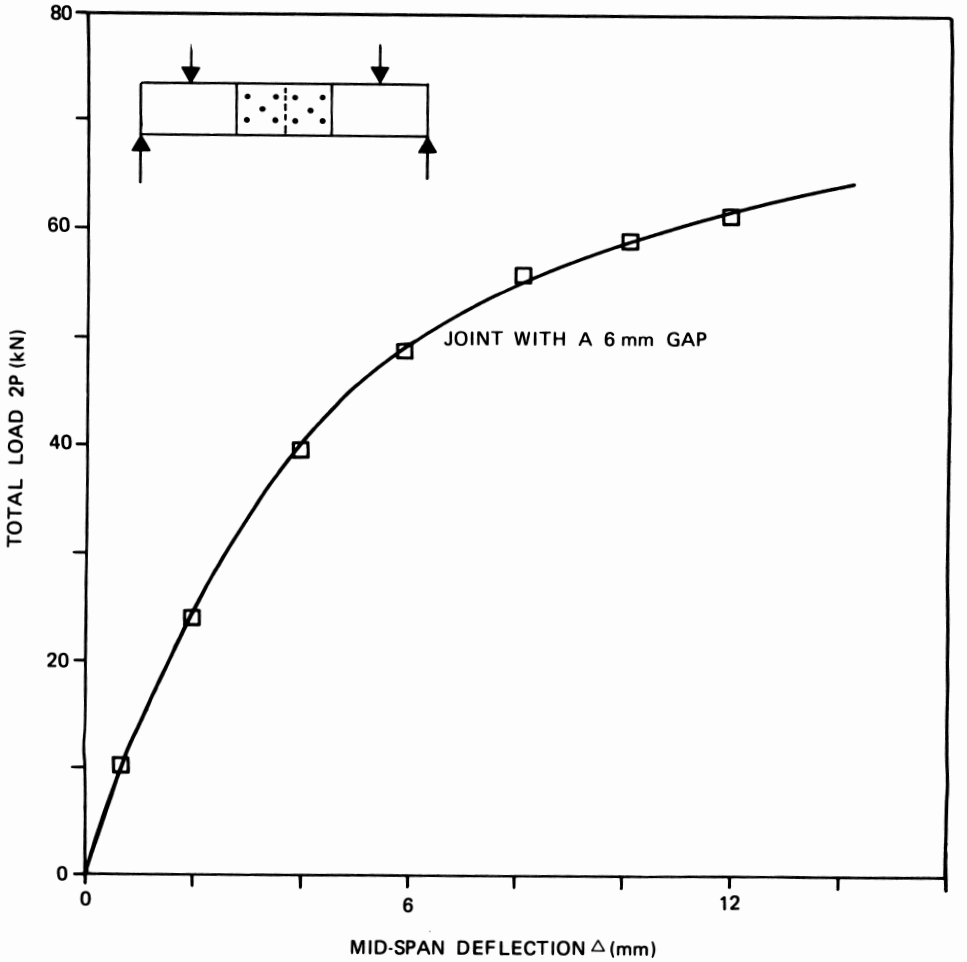

Figure 6. Average test load/mid-span deflection for joints with a 6-mm gap at mid-span.

different points ranged from 5 to 12%. There was a nonlinear relationship between the joint lateral load and the mid-span deflection due to shear, elastic deformation of the lumber, and the differential rotation between the lumber members and the gussets. This curve which represents the lateral load applied to the joint versus the joint deflection must be modified to consider only deflection due to joint rotation.

The conjugate beam method was used to correct for shear and bending deformation of the lumber members and to express the test results as joint moment versus joint rotation. Shear and bending deformation contributed to 1/10 of the total deflection. Figure 7 shows the average of the moment-rotation curves for the test specimens as well as the theoretical moment-rotation curve.

The curves have similar shapes and show a nonlinear relationship between the bending moment and joint rotation. Variation between the curves is smaller than the variability expected in wood. The theoretical flexural formula can then be used to estimate the rotational stiffness of a multi-laminated nailed joint.

Effects of axial and shear forces

Theoretical

In a full-scale truss, a bending moment rarely occurs alone; it is often combined with axial and shear forces. The shear forces are small even when the joints are perfectly rigid and their effects can be neglected. But the axial forces are large and their effect on the rotational resistance may not be negligible.

Massé (1985) reported a theoretical investigation to determine the effect of axial and shear forces on rotational stiffness. When axial, shear and bending moment forces act on a joint, each nail has to resist force components in the direction of shear and axial forces and another component due to bending moment. Figure 8 shows the force components on the nails.

When all the individual forces on each nail are known, their resultant force can be determined. The new center of rotation of the nailing pattern must be located at the intersection of the lines extending perpendicularly from the resultant force at each nail. When bending moment acts alone on a joint the center of rotation is located at the center of resistance of the nailing pattern. But when axial and shear forces are present with bending, the center of rotation will move away from the center of resistance.

The following formulae developed by Massé (1985) give an approximation of the horizontal and vertical translation of the center of rotation from the center of resistance and also give the joint rotation around the center of rotation.

$$\Delta x = \frac{\sum_{i=1}^{n} K_i^s \bar{x}_i - \frac{Fv}{\theta}}{\sum_{i=1}^{n} K_i^s}$$

$$\Delta y = \frac{\sum_{i=1}^{n} K_i^s \bar{y}_i + \frac{Fx}{\theta}}{\sum_{i=1}^{n} K_i^s}$$

$$\theta = \frac{M + Fx\,\Delta y - Fv\,\Delta x}{\sum_{i=1}^{n} K_i^s R_i^2}$$

where

Δx = horizontal displacement of the center of rotation (mm),
Δy = vertical displacement of the center of rotation (mm),
θ = joint rotation (radian),
K_i^s = modulus of displacement (N/mm),
$\bar{x}$ = horizontal nail distance from the center of resistance (mm),
$\bar{y}$ = vertical nail distance from the center of resistance (mm),
Fx = joint axial force (N),
Fv = joint shear force (N),
M = joint moment (N.mm), and
R_i = distance of the nail from the center of rotation (mm).

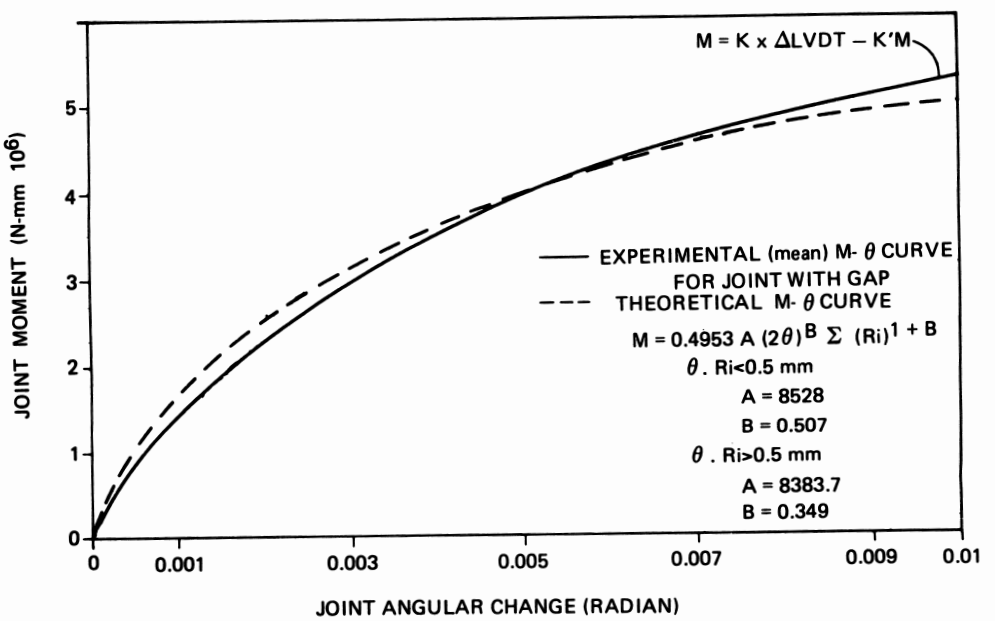

Figure 7. Theoretical and mean experimental moment/rotation curve of joints tested in bending.

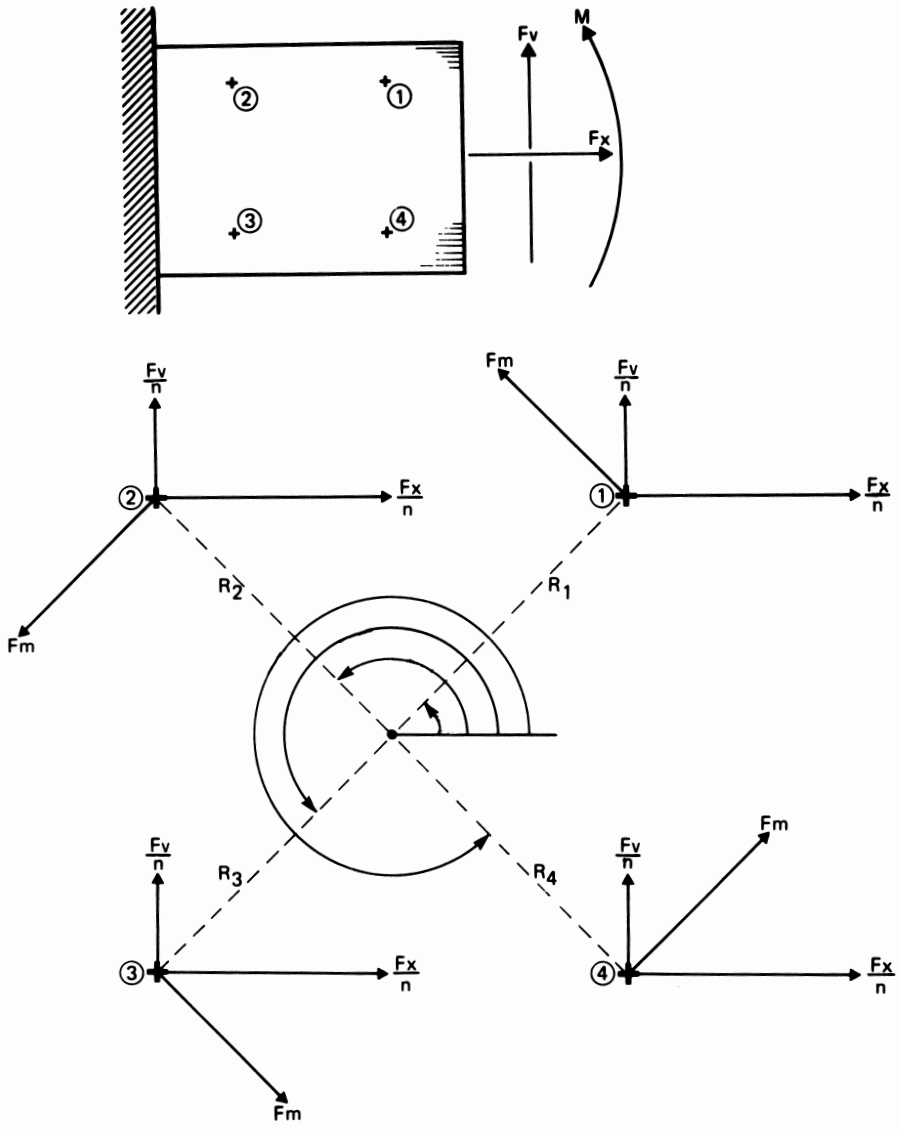

Figure 8. Force components on a nail due to axial, shear and bending moment forces.

There are three equations and three unknowns, therefore an iteration procedure is used to determine θ, Δx and Δy. The first step is to determine θ assuming that the known moment acts alone on the joint; when θ is known then Δx and Δy are determined and a new value for θ can then be found. Iterations are continued until the θ, Δx and Δy values converge.

Experimental

An experimental investigation of the rotational stiffness of a multi-laminated nailed joint under the action of axial force and bending moment was carried out to verify the adequacy of the above theoretical analysis and also to determine if the effect of axial forces on the rotational stiffness is, by itself, an important enough factor to be included in the analysis.

Twenty specimens were built identical to those tested in bending (Fig. 9). At both ends of the specimen, 4.8-mm steel plates were epoxy-glued on both sides of the double members and fastened with four 12.5-mm bolts. This provided a strong, rigid connection to eccentrically load the specimen. The joint rotation was measured by LVDT no. 1 and no. 2, while joint deflection by LVDT no. 3.

Tests were conducted on ten joints with an eccentricity of 40 mm, and on 10 joints with an eccentricity of 80 mm to develop simultaneously variable axial and bending moment forces in the joint. The conjugate beam method was used to subtract the joint deformations due to elastic deformation of the wood. The corrected results were expressed as joint moment versus joint rotation. Figure 10 shows the theoretical and mean experimental moment-rotation relationships of the joints tested in tension with different eccentricities. The coefficient of variation for each series ranged from 4 to 14%.

The theoretical and experimental results are in good agreement and show that the axial force has a significant effect on the rotational stiffness of the joint. When axial force increases the rotational stiffness decreases. Because of the good agreement observed, the proposed theoretical approach was then used to analyze the effect of axial forces on the rotational stiffness of joints on full-scale trusses.

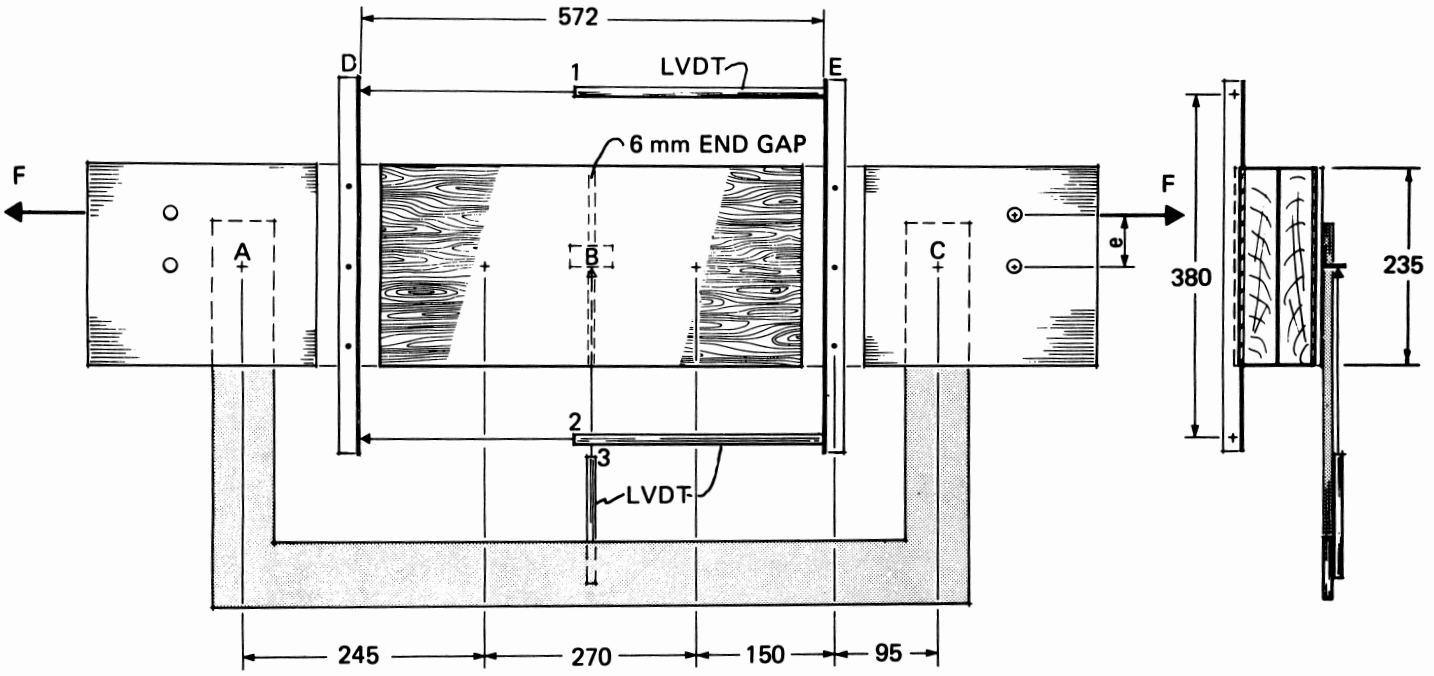

Figure 9. Details of test specimen under tension and bending moment forces (dimensions in mm).

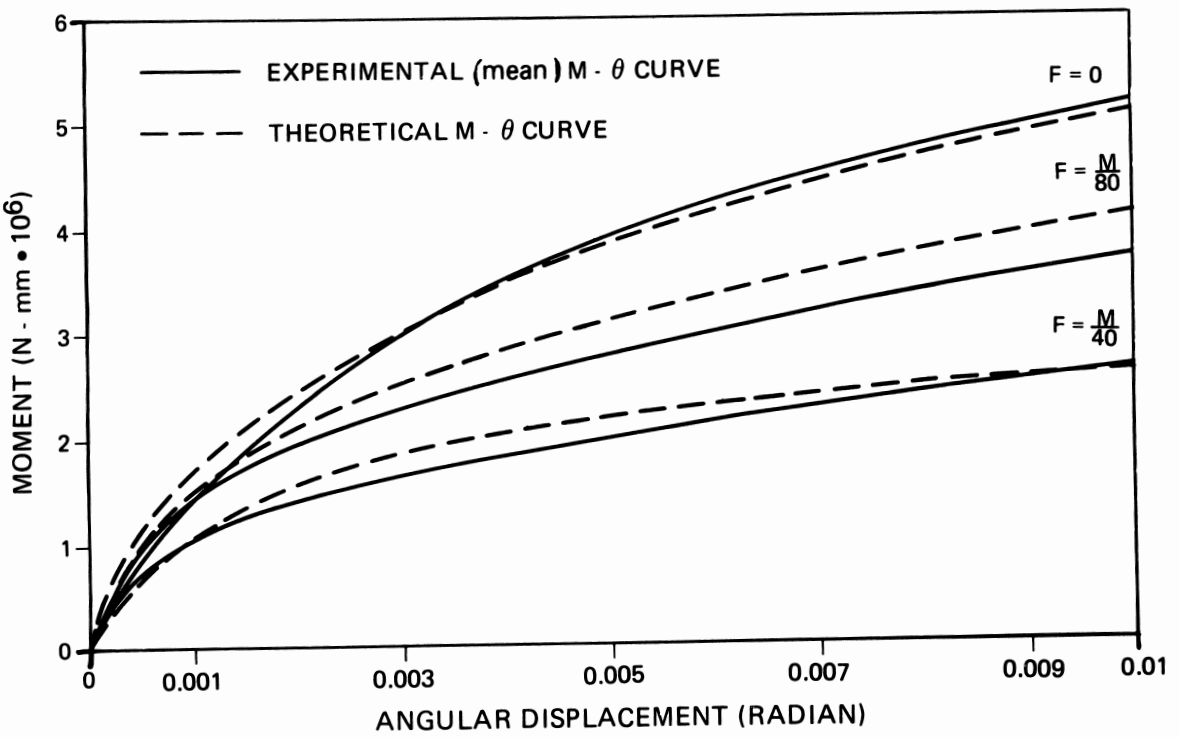

Figure 10. Theoretical and mean experimental moment/ rotation curve for different values of the axial forces (Massé 1985).

ANALYSIS OF FULL-SCALE TRUSSES

Theoretical

The results of the above investigation were used to predict more accurately the internal axial, shear and bending moment forces and also to predict the deflected shape of full-scale trusses. Figure 11 shows the multi-laminated nailed joint truss configuration analyzed. In-plane loading was used to simulate the testing apparatus loading system. Also shown in Fig. 11 are the joint configuration and construction details.

The truss was analyzed for three different joint conditions: joints assumed pinned, joints assumed rigid, and joints assumed to have some axial and rotational stiffness. Figure 12 shows the

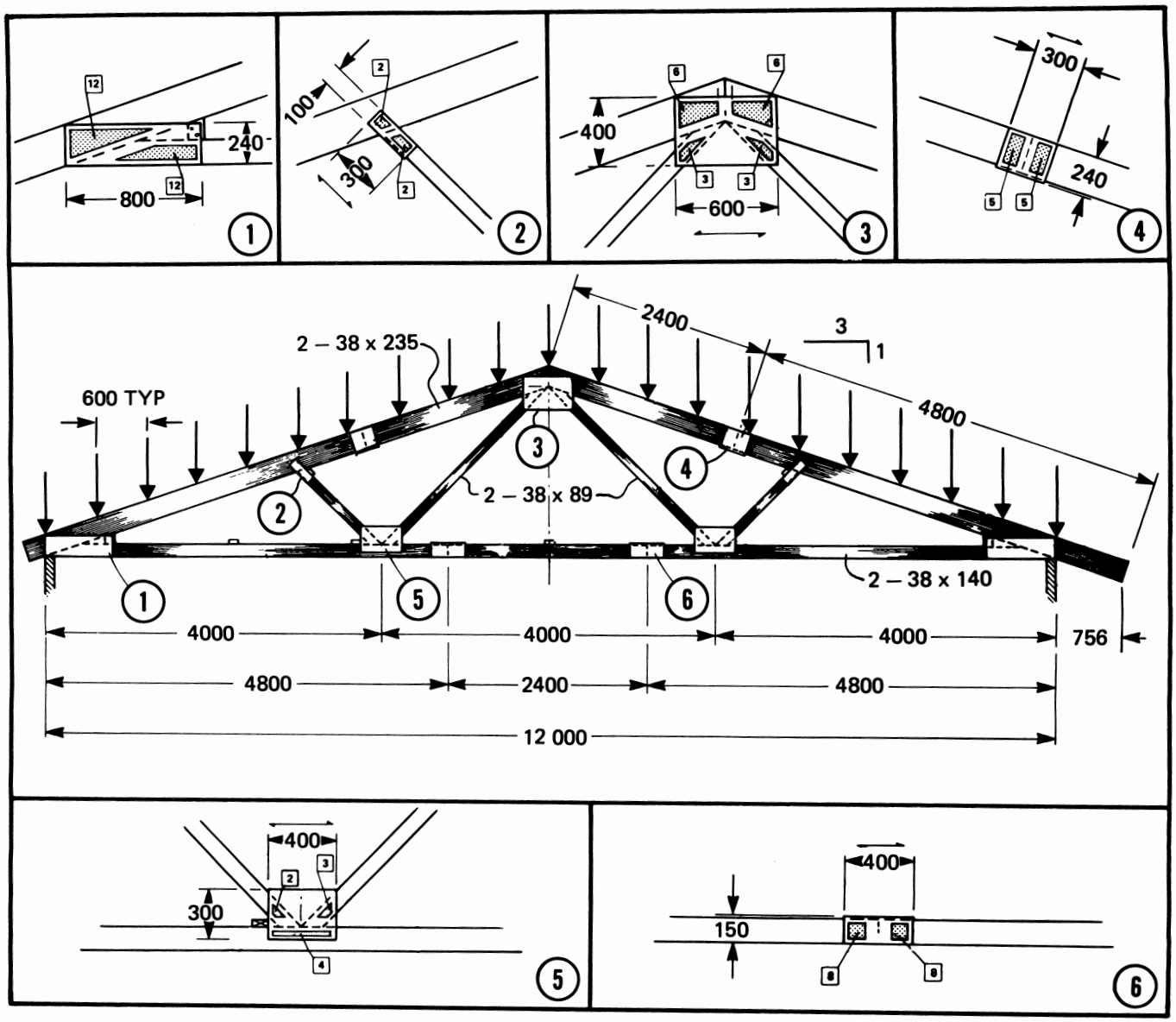

Figure 11. Truss configuration and geometry (numbers in circles denote the joint number and numbers in squares denote the number of nails in each side of the joint).

truss analog model for the pinned and rigid joint condition and Fig. 13 shows the analog model for trusses with semi-rigid connections which is a more realistic representation of the structure. The nailing pattern axial and rotational stiffnesses are represented in the model by using a short fictitious member having a cross-sectional area and moment of inertia equivalent to the joint's axial and rotational stiffness, respectively (Massé 1985).

For most connections (except the heel joint) the member centerlines met at almost the same point, and in order to simplify the analysis it was assumed that there were no eccentricities. The heel joints, however, were built with large size upper and lower chords with center lines that did not meet at the reaction line. At that location the eccentricity cannot be ignored and should be included in the analysis by using a short member having a length equal to the eccentricity and having a large axial and rotational stiffness.

To model the effective length of each chord splice, a fictitious member was introduced in the analog model. This member had the same axial and flexural stiffness as the gussets.

The truss was analyzed for two roof loads corresponding to half and full design load.

For the analog models with the pinned and rigid joints, the analyses were carried out in one operation. For the analog model with semi-rigid connections the analysis was nonlinear since the stiffness of the structure was a function of the applied load. Several steps were necessary to carry out the analysis.

The first step was to determine the moment-rotation relationship of the connections including the effect of axial forces and also to determine the axial force-displacement relationship of the joint. Figures 14 and 15 show the heel joint upper chord connection and the corresponding load-displacement relationships; similar relationships were developed for all the joints in the truss.

The second step was to calculate the first estimate of forces at the member end. These were found by assuming that the axial and rotational joint stiffnesses were equal to the slope of the tangent at the origin of the load-deformation curves. They are

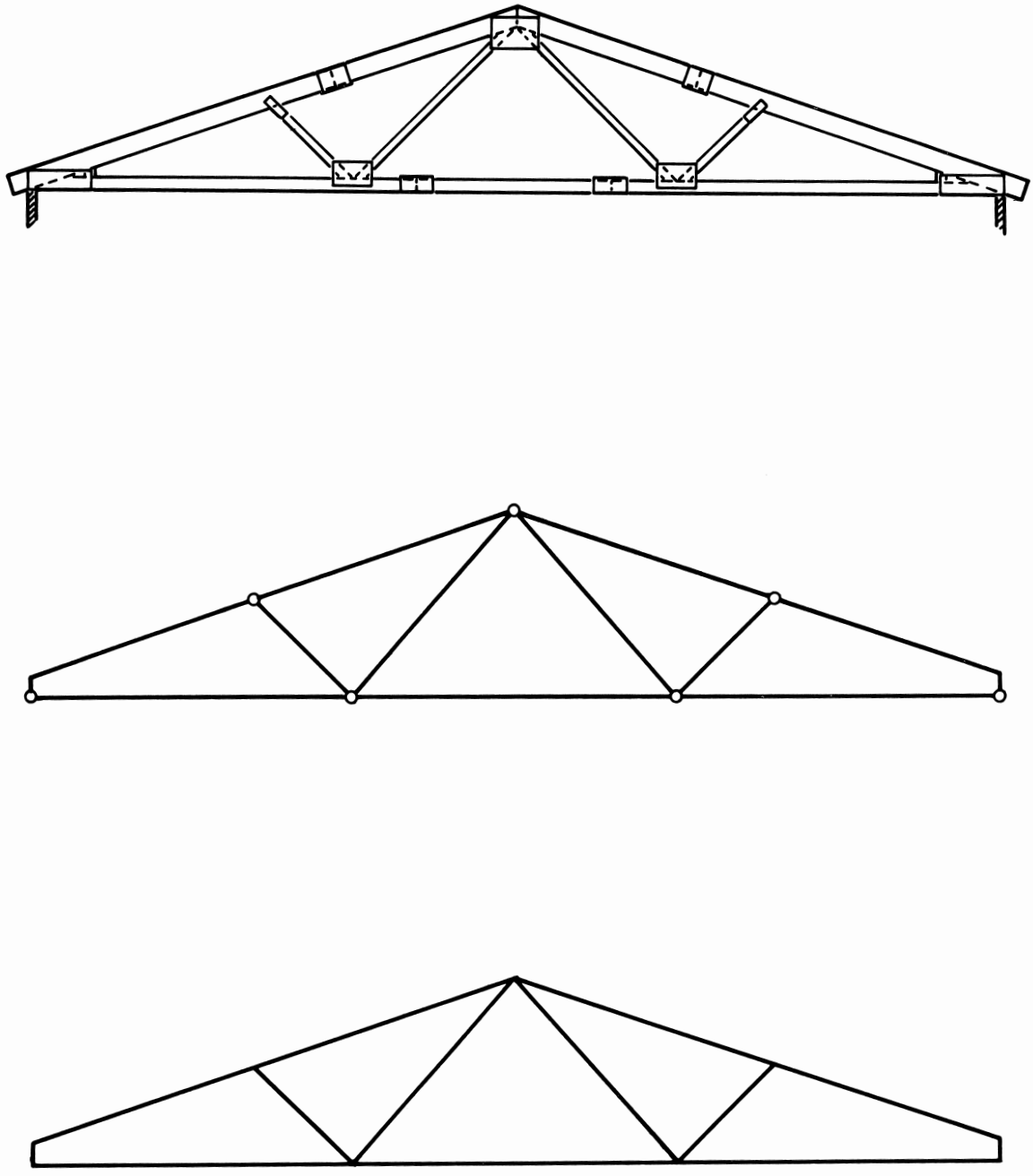

Figure 12. Analog model for pinned and rigidly connected trusses.

shown as parameter K_{A1} and K_{B1} in Figs. 14 and 15 for the heel joint upper chord connection.

The third step was to determine the moment of inertia and the cross-sectional area of the short fictitious member simulating the joint. The analytical procedure is given in Appendix A.

The fourth step was to use the first estimate of forces to determine new values for the joint's axial and rotational stiffness, K_{B2} and K_{A2}. Figures 14 and 15 show these new values for the heel joint upper chord connection.

Iterations were continued until values of the axial and rotational stiffness converged (typically after three iterations). The structural analysis was carried out using SPAM (Carleton University Space Frame Computer Structural Analysis Program).

The axial forces found with the rigid joint model were the highest while those found using the semi-rigid joint models were the lowest, but the variation in axial forces from one model to the other was less than 5%.

As shown in Fig. 16, at the heel joint location the difference in bending moment between analog models with rigid and semi-rigid joints was very small, while at the ridge joint the difference was large. This is because the connection at the ridge has few nails and a low rotational stiffness. The partial rigidity of the ridge joint increases the bending moment in the upper chord at the location of the web connection.

Tables I and II compare the maximum bending moments, axial forces and combined stress ratio in the upper and lower

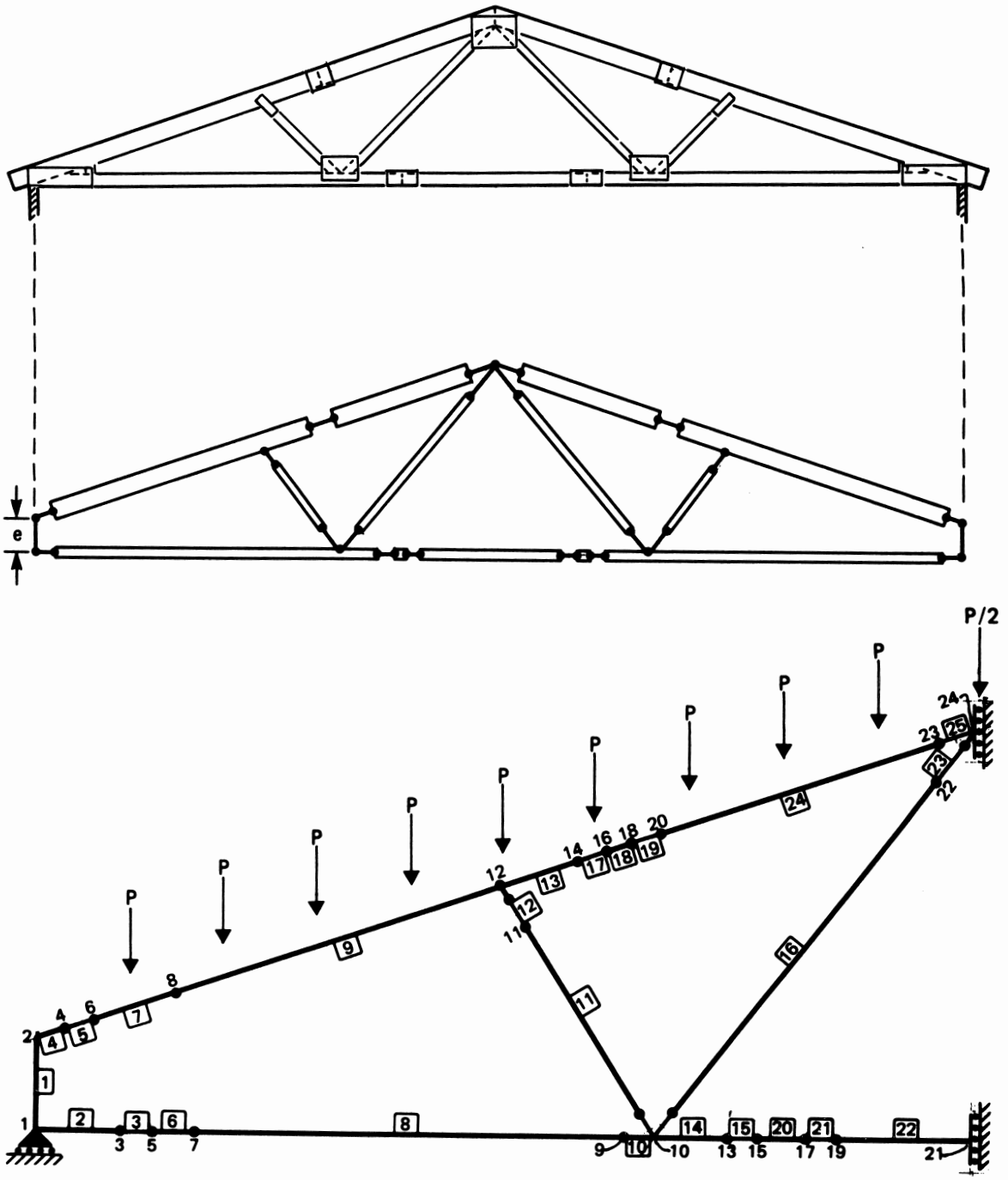

Figure 13. Analog model for truss with semi-rigid connections.

Table I. Comparison of upper chord forces, moments and stress ratios found with the traditional and refined analysis methods

Item	Traditional analysis method	Refined analysis method
F (N)	57900	54656
M (kN − m)	3.93	2.08
Combined stress ratio $\frac{M}{S\times F'_b}+\frac{P}{A\times F'_c}$	0.97	0.74

Table II. Comparison of lower chord forces, moments, and stress ratios found with the traditional and refined analysis methods

Item	Traditional analysis method	Refined analysis method
F (N)	550900	50825
M (kN − m)	0.00	0.32
Combined stress ratio $\frac{M}{S\times F'_b}+\frac{P}{A\times F'_c}$	0.69	0.79

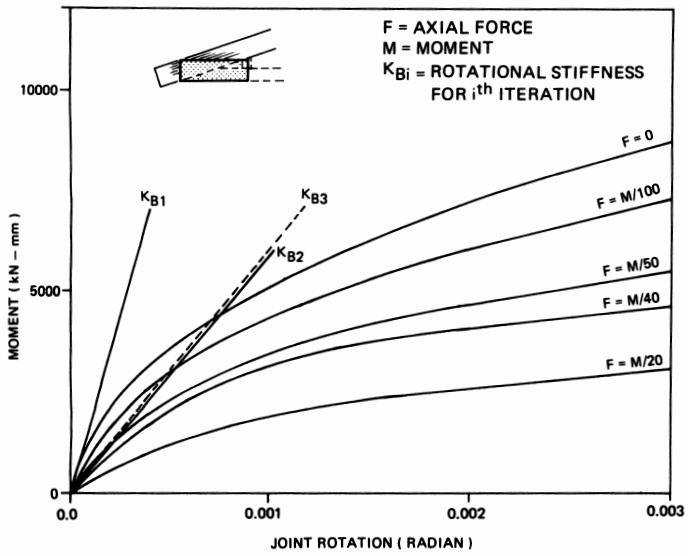

Figure 14. Moment/rotation curves, heel joint upper chord connection.

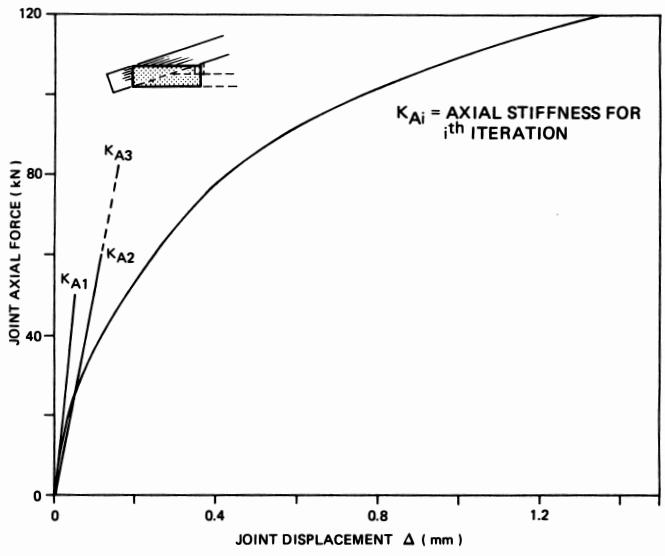

Figure 15. Load/deformation curve, heel joint upper chord connection.

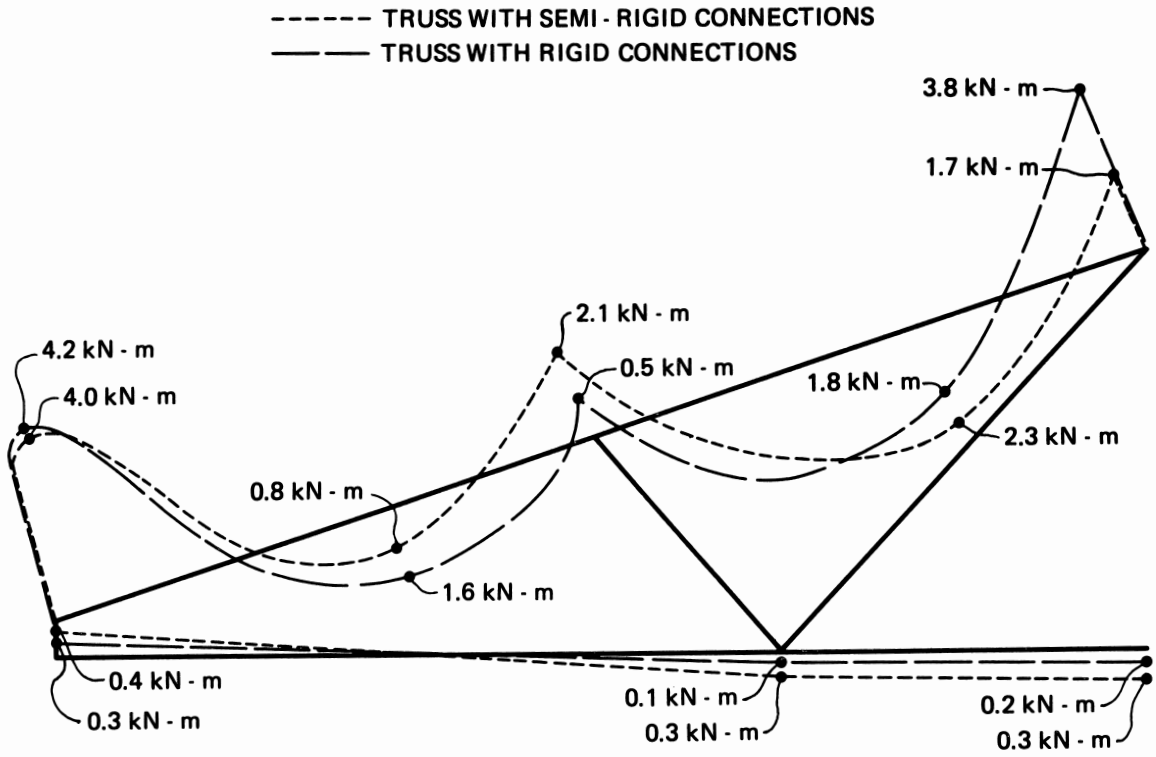

Figure 16. Moment distribution within the truss for different joint fixity conditions.

chords of the truss analyzed using the traditional and the more refined structural analyses. These tables show that the axial forces in upper and lower chords estimated with the refined analysis method are smaller than those determined with the traditional method. The same applies to the top chord moment. The bottom chord has, of course, no moment using the traditional method and a small bending moment using the refined method. The combined stress ratios calculated from the axial force and moment for top and bottom chords are about equal when the refined method is used for analysis. In theory, the failure should occur at random in the lower and upper chord exterior spans. But in reality, the maximum stress in the upper chord is concentrated near the web connection and the heel joint. In the lower chord, the maximum stress occurs throughout the exterior span. Therefore the probability of having lumber defects in the region of maximum stress is higher for the lower chord than for the upper chord. Also, lumber defects would be more critical for the lower chord because all the fibers are in tension. It is thus more probable for a lower chord failure to occur than an upper chord failure. This may explain why there were no upper chord failures in the full-scale truss tests.

Experimental

An experiment was carried out to verify the adequacy of the refined analysis method presented in the previous section. Five trusses were fabricated with No. 2 S-P-F lumber and assembled with multi-laminated nailed joints. The trusses were built using the same procedure as the joints previously tested.

The trusses were tested one at a time in a horizontal position with the load applied by a cable and pulley system. This testing facility had been developed by Turnbull et al. (1983b). Figure 17 shows the test setup and the locations of the displacement potentiometers used to measure the truss deformation. The ridge joint, the lower chord mid-span and lower chord web member connection deflections were measured as well as both heel joint deformations. These deformations were then compared with those predicted with the truss analog model using semi-rigid joints or pinned joints.

Tables III and IV compare the calculated and the average measured deflections. As shown, the refined analysis method is in better agreement with the experimental results than the traditional method. The variations between the experimental deflections and those predicted using the refined analysis method were small and within the range normally expected with wood.

It was also found that truss deflections were not significantly affected by the rotational stiffness of the joint but were mainly due to lumber member and joint axial deformation.

Table V shows the comparison between the calculated and measured heel joint deformations. Good agreement was obtained between the theoretical and experimental results. The calculated rotational stiffness (a function of the heel joint axial forces) represented a good analog model of the real truss.

Table III. Comparison of deflection at specific points at 0.5 design load

Location	Predicted deflection: Traditional analysis method (mm)	Predicted deflection: Refined analysis method (mm)	Experimental deflection (mm)	
Ridge joint	7.6	9.2	m†	10.8
			CV†	8%
Center of lower chord	7.7	11.3	m	12.5
			CV	5%
Lower chord web connection	7.6	9.2	m	10.9
			CV	9%

†m is the mean deflection; CV is the coefficient of variation.

Table IV. Comparison of deflection at specific points at 1.0 design load

Location	Predicted deflection: Traditional analysis method (mm)	Predicted deflection: Refined analysis method (mm)	Experimental deflection (mm)	
Ridge joint	15.1	21.5	m†	24.2
			CV†	13%
Center of lower chord	15.4	26.2	m	28.7
			CV	8%
Lower chord web connection	15.2	21.5	m	24.6
			CV	10%

†m is the mean deflection; CV is the coefficient of variation.

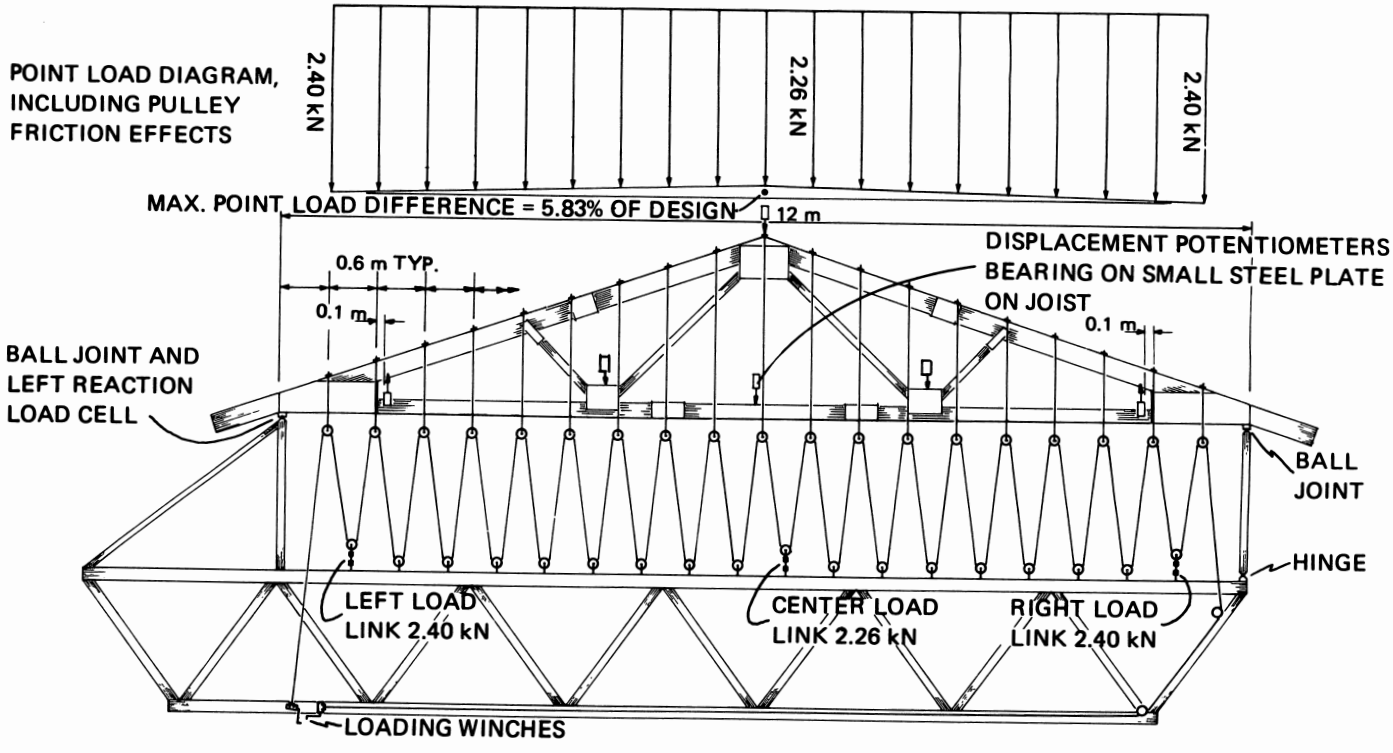

Figure 17. Loading plan for series of truss tests, truss plan M-9231, design load 1.7 kN/m² on roof trusses spaced at 2.4 m.

Table V. Comparison of calculated and measured heel joint deformation at two different roof loads

Roof load (design load)	Predicted heel joint deformation† (mm)	Measured heel joint deformation (mm)	Ratio (%)
0.5	0.68	0.73	0.93
1.0	1.64	1.96	0.84

†Refined analysis method.

With the stiffness method of structural analysis, the truss member end forces are calculated by using the joint rotation and deflection. Because of the good agreement between the calculated and measured heel joint deformation and truss deflection, the real member forces can be determined with the same accuracy.

The truss failures occurred at random in the lower chord, as was expected. Thus, the proposed design method, which considers the interaction between the joints and member stiffness, is more accurate than the previous design methods.

CONCLUSIONS

The design procedure proposed determines with good accuracy the axial and rotational stiffness of a multi-laminated nailed joint and achieves a more precise analysis of multi-laminated nailed joint trusses.

Good agreement was obtained between the theoretical and experimental joint stiffness behavior, and between the analog model using semi-rigid joints and the full-scale truss tests.

Because of the good agreement obtained, the calculated truss member forces are expected to be a better representation of the actual member forces.

The new design method is more accurate than the previous method based on traditional design assumptions which overdesign the upper chord and underdesign the lower chord joints.

ACKNOWLEDGMENT

Appreciation is expressed for valuable suggestions made by J. E. Turnbull, Director of the Canada Plan Service (CPS) Design Center of Agriculture Canada and for technical support by Bob Ellis of Carleton University and Don Lowe of Agriculture Canada. Also, thanks are expressed to Carleton University for providing the Civil Engineering Structural Laboratory and the Computer Services Facilities.

REFERENCES

ANONYMOUS. 1977. Canadian farm building code, NRCC no. 15564, National Research Council of Canada, Ottawa, Ont.

ANONYMOUS. 1980a. Code for engineering design in wood. National Standard of Canada CAN3-086-M80, Canadian Standards Assoc., 178 Rexdale Blvd., Rexdale, Ont.

ANONYMOUS. 1980b. Load test procedure for wood roof trusses for houses and small buildings. CSA Standard S307-M1980, Canadian Standard Assoc., 178 Rexdale Blvd., Rexdale, Ont.

GERHARDS, C. C. 1980. Effect of moisture content and temperature on the mechanical properties of wood: an analysis of immediate effects. U.S. Forestry Service Paper No. 2079. U.S. Dept. Agr. Forest Products Laboratory, Madison, Wis.

MASSÉ, D. I. 1985. Design and analysis of multi-laminated nailed joint trusses. M. Eng. Thesis, Dept. of Civil Engineering, Carleton University, Ottawa, Ont. 174 pp.

PERKINS, R. H., A. C. DALE, and S. K. SUDDARTH. 1962. Rotational resistance of three membered nailed joints subjected to bending movement. Perdue University Agric. Exp. Sta. Res. Bull. no. 753.

RODDA, E. D. 1967. Analysis of indeterminate nailed structures. Forest Products Laboratory 168, Madison, Wis.

SUDDARTH, S. K. 1961. Determination of member stresses in wood trusses with rigid joints. Purdue Univ. Agric. Exp. Sta. Res. Bull. No. 714.

TURNBULL, J. E., L. P. LEFKOVITCH, and D. L. LOWE. 1981. Multi-laminated nailed truss connections. Can. Agric. Eng. 23(2): 113–119.

TURNBULL, J. E., D. I. MASSÉ, and D. J. BUCKLEY. 1983a. First experiences with a new facility for testing wood-framed roof trusses, diaphragms and rigid frames. Can. Agric. Eng. Vol. 25(1): 101–109.

TURNBULL, J. E., D. I. MASSÉ, L. P. LEFKOVITCH, and D. L. LOWE. 1983b. Performance of single-member versus double-member gable roof trusses. Can. Agric. Eng. 26(2): 227–232.

TURNBULL, J. E., L. P. LEFKOVITCH, and D. L. LOWE. 1983c. Single-slope doubled truss performance with nailed triple gusset plates. Can. Agric. Eng. 26(2): 219–225.

APPENDIX A

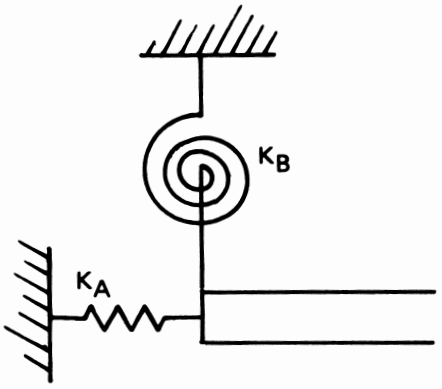

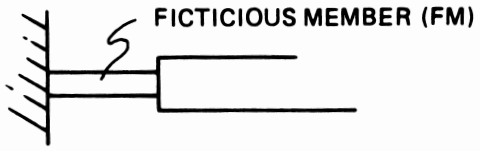

CROSS SECTION "A" OF (FM)

$$P = \frac{EA}{L}\Delta$$

$$\frac{P}{\Delta} = \frac{EA}{L} = K_A$$

THEREFORE $A = \frac{K_A L}{E}$

MOMENT OF INERTIA "I" OF (FM)

$$M = \frac{EI\theta}{L}$$

$$K_B = \frac{M}{\theta} = \frac{EI}{L}$$

THEREFORE $I = \frac{K_B L}{EI}$